Structural/Physicochemical Properties of Corycavidine, a Key Intermetabolite in the Biosynthesis of Isoquinoline Alkaloids, Elucidated by X-Ray Crystallography, Solution Conformation and Thermal Behavior Analyses, and Energy Calculations

Miyoko Kamigauchi,* Mayumi Yoshida, Kayoko Saiki, Makiko Sugiura, Jujiro Nishijo, Yasuko In,† and Toshimasa Ishida†

Department of Physical Chemistry, Kobe Pharmaceutical University, 4-19-1 Motoyama-kitamachi, Higashinada-ku, Kobe 658-8558

†Osaka University of Pharmaceutical Sciences, 4-20-1 Nasahara, Takatsuki, Osaka 569-1094

(Received October 14, 1999)

The conformational/physicochemical features of corycavidine (**1**), 5,7,8,15-tetrahydro-3,4-dimethoxy-6,15-dimethyl-[1,3]benzodioxolo[5,6-*e*] [2]benzazecin-14(6*H*)-one, an important protopine-type alkaloid that serves as the key intermetabolite in the biosynthesis of isoquinoline alkaloids, were examined by X-ray crystallography, ^{1}H NMR spectroscopy, as well as thermal analysis and energy calculations. Two stable conformations of **1**, as proposed by energy calculations, were also observed in both the crystalline and solution states. Racemization of optically active **1**, which was caused by heating of the crystal, was analyzed by differential-scanning calorimetry. By taking advantage of the H–^{2}H replacement reaction at the C13 atom of **1**, the rate of racemization in the $C^2H_3O^2H/NaO^2H$ solution was measured as a function of the temperature; the energy barrier between both enantiomers was estimated to be 4.7 kcal mol^{-1}. The crystallization of racemic **1** led to two different crystal forms, i.e., the racemic crystal and the conglomerate crystal (1 : 1 mixture of both enantiomeric crystals). This was probably due to the low energy difference between both crystals. These physicochemical behaviors are important for understanding the in vivo nonenzymatic racemization of **1** and its related alkaloids during metabolic processes.

Clarification of the absolute structure of a metabolite in a biosynthetic pathway is important for understanding its chemical stability and the variation of its biochemical function. In our structural analyses of metabolites which participate in the biosynthetic pathway of hexahydrobenzo[*c*]-phenanthridine-type alkaloids,[1] we have reached a hypothesis that the racemization behavior of corycavidine (**1**), which is a protopine-type alkaloid and is an intermetabolite of protoberberine-type alkaloids (Fig. 1), may be strongly related to the selection of different metabolic routes. In order to confirm our hypothesis, it is important to elucidate the racemization process, as well as the structural/physicochemical behaviors of **1** enantiomer and racemate.

Therefore, in this paper we deal with the chemical and conformational properties of **1** in the crystalline and solution states, as studied by X-ray crystallography, ^{1}H NMR spectroscopy, differential scanning calorimetry (DSC)/thermogravimetry (TG), and energy calculations. The chemical structures of **1** and related metabolites **2**—**4**, together with the atomic numbering[2] for **1**, are given in Fig. 2.

Results

Preparation of (−)-1. The chemical synthesis of **1** has not yet been established, and only the isolation of (+)- and (±)-**1** from *Corydalis cava* (*Papaveraceae*) has been reported so far.[3,4] Thus, it is important to establish a biotransformation method using plant cells to obtain optically active **1**. By referring to a previous report[5] on the biosynthesis of (−)-**2** from (±)-*N*-methyl-*meso*-tetrahydrocorysaminium ((±)-**3**) using the callus of *C. incisa*, the biotransformation of (±)-*N*-methyl-*meso*-thalictricavinium ((±)-**4**) to (−)-**1** was attempted using several cells; the callus tissues of *Chelidonium majus* (*Papaveraceae*) were finally used.

The callus tissues of *C. majus* were derived from the seedling root, and the substrate of (±)-**4** chloride, which was labeled by carbon 13 to estimate the degree of incorporation, was administered according to a previous procedure.[6] Consequently, (±)-[N–$^{13}CH_3$]-**4** salt was transformed to levorotatory (−)-[N–$^{13}CH_3$]-**1** with 100% optical purity and a conversion yield of 4.25%. The 13*R* configuration of (−)-**1** was determined by a comparison of its CD band pattern with that of (−)-**2**; the 13*R* configuration of (−)-**2** was chemically[7] and crystallographically[5] determined. The CD spectra of (−)-**1** and (+)-**1** in methanol are shown in Fig. 3.

Thermal Analysis of 1 Crystal. To determine in detail the mechanism involved in the racemization of **1** enantiomeric crystals, the thermal behavior of (−)-**1** crystals was analyzed by DSC/TG. The thermal profile is shown in Fig. 4,

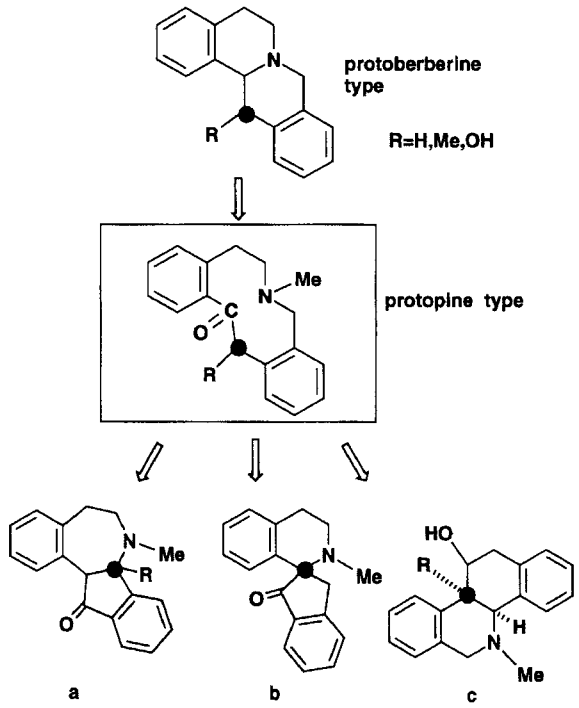

Fig. 1. Biosynthetic pathway of protoberberine-type alkaloid to three different alkaloids via the protopine-type intermediate. a; benzindanoazepine (benz[*d*]indan[1,2-*b*]azepine) type. b; spirobenzylisoquinoline (spiro[indan-2-1′-isoquinoline]) type. c; hexahydrobenzo[*c*]phenanthridine type.

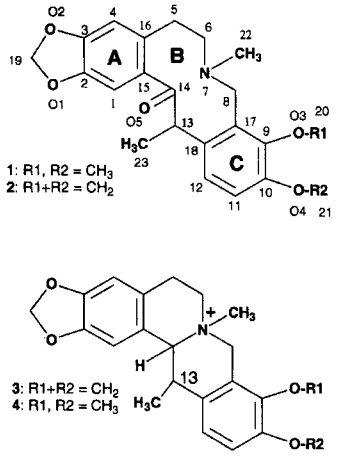

Fig. 2. Chemical structures of **1**—**4**, together with the atomic numbering[2] of **1**.

where the DSC curve in the range of 50 to 225 °C is designated as State I, and State II corresponds to the DSC profile of the same crystal sample, which was once completely melted by heating to 230 °C and then cooled to room temperature. The TG curve showed no weight loss of the sample during heating to 230 °C.

(−)-**1** began to melt at 209 °C and the majority of crystals melted at approximately 210 °C (Fig. 4(a)). When the crystals were melted completely and then cooled to room temperature, a new solid phase of State II appeared, which showed a different X-ray diffraction pattern from State I (data not shown). The DSC profile of this solid phase showed melting at 195 °C (Fig. 4(b)). As judged from the respective melting points, the endothermic Peaks I (T_{max} = 210.8 °C, ΔH = −49.37 kJ mol^{-1}) and II (T_{max} = 195.1 °C, ΔH = −38.07 kJ mol^{-1}) agree well with the melting processes of (−)-**1** and (±)-**1**,[3,4] respectively. It is clear that (i) Peak I reflects the heat of melting of (−)-**1** plus heat of racemization to (±)-**1**, while Peak II reflects only the heat of melting of (±)-**1**; (ii) State II corresponds to the DSC profile of (±)-**1** crystal; (iii) the two states are irreversible; and (iv) the crystal of State II is energetically less stable than that of State I.

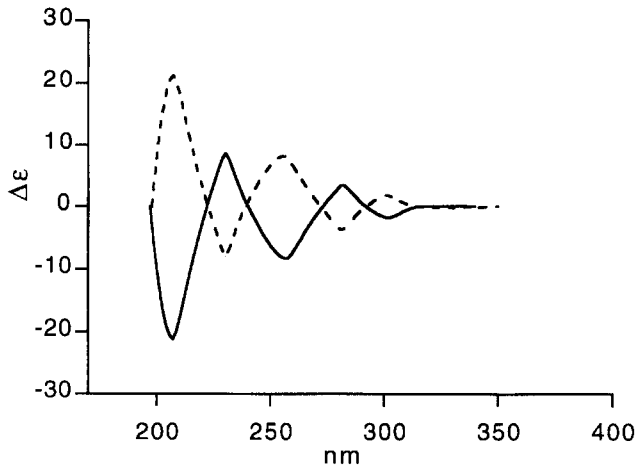

Fig. 3. CD spectra of (−)-**1** (——) and (+)-**1** (- - -) in methanol.

Polymorphic Behavior of 1 Crystal. In general, it is known that a racemic crystal tends to have a higher melting point than an optically active one, due to the energetically favorable centrosymmetric molecular packing allowed only for the former. However, (±)-**1** crystals showed a lower melting point (mp 193—195 °C) than (+) or (−)-**1** crystals (mp 212—213 °C), which implied that the former crystal was less stable than the latter one. This crystal behavior of **1** was characterized by the following crystallization experiment.

When an acetone solution of (±)-**1** was allowed to stand at room temperature (22±3 °C), two different solid forms, needlelike crystals ((±)-**1n**, mp 193.2—194.0 °C) and prismatic clusters ((±)-**1p**, mp 209.0—210.0 °C), appeared over the course of several days, while only prismatic crystals were obtained from the solution of (−)-**1** or (+)-**1**. As judged from the melting point, the crystals of (±)-**1n** could be racemic **1** crystals, in which two enantiomers are present in equal quantities in a unit cell. On the other hand, the value and signs of the optical rotation for each particle, which were obtained by dividing the (±)-**1p** cluster into 31 particles with the aid of a microinjection needle under a microscope, indicated that it is a "conglomerate crystal",[8] i.e., a mechanical mixture of two pure (−)-**1** and (+)-**1** crystals.[9]

Crystal Structures and Molecular Conformations of (−)-1 and (±)-1. The molecular conformations of (−)-**1** and (±)-**1** are shown in Figs. 5(a) and 5(b), respectively. Their overall features are similar. The methoxy groups attached to the C9 and C10 atoms are at right angles and parallel to aromatic ring C, respectively. Such a twisting could be

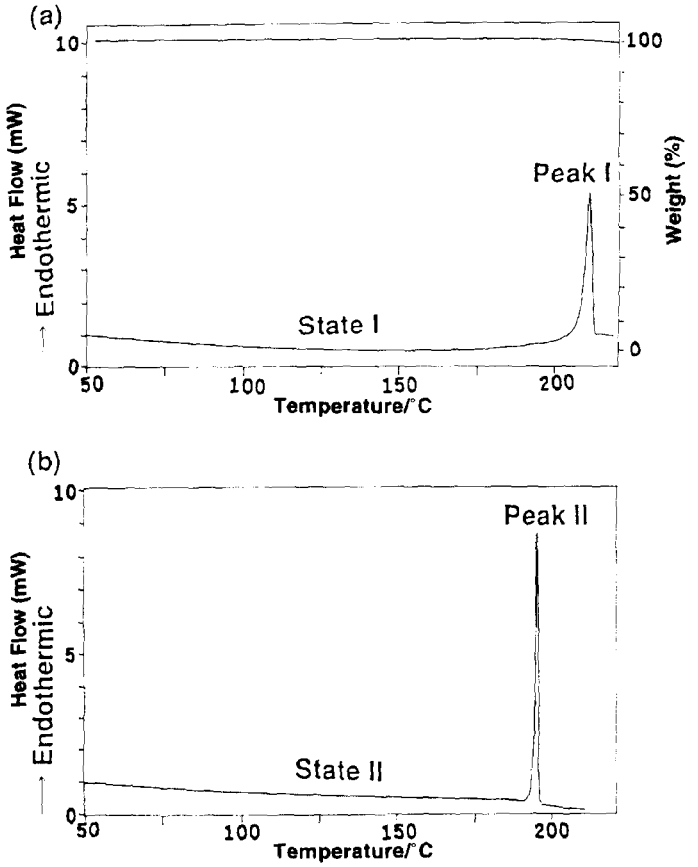

Fig. 4. DSC/TG profiles of (−)-**1** crystals. States I (a) and II (b) represent DSC profiles of the newly prepared crystals of (−)-**1** and of the same (−)-**1** crystals which were first heated to 230 °C and then cooled to room temperature, respectively. The upper line of (a) corresponds to the TG profile of (−)-**1** crystals. The same TG profile is also observed for (b).

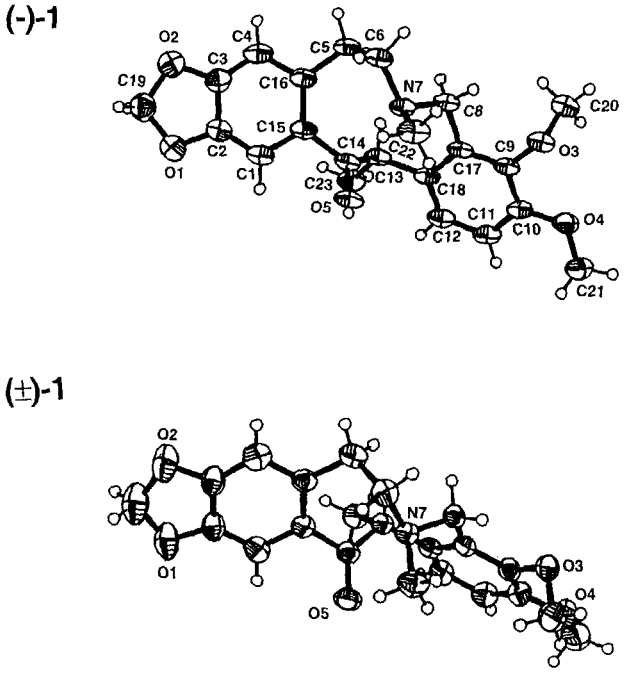

Fig. 5. Molecular conformations of (−)-**1** and (±)-**1**n molecules. The ellipsoids are drawn at 50% probability. Circles representing hydrogen atoms are arbitrarily shown.

due to a steric repulsion caused by the steric hindrance between C(8)H_2 and C9 methoxy group. The dihedral angle between rings A and C is 36.9(5)° for (−)-**1** and 43.7(5)° for (±)-**1**; thus, **1** has an open conformation. In the molecular structure, the carbonyl group is located on the β side and an electrostatic interaction with the N7 lone pair on the α side is observed [N7–C14 = 2.443 Å for (−)-**1** and 2.464(2) Å for (±)-**1**]. Although this value is slightly smaller than that of (−)-**2** (2.554 Å[10] or (±)-**2** (2.618 Å),[11] the observed open conformation between them is basically identical. Thus, such an open conformation is generally suitable for the 13-methyl protopine-type alkaloid.

As is obvious from this figure, the torsion angles around the C17–C9–O3–C20 (ω) bond differ from each other [−89.4(2)°for (−)-**1** and 103.4(2)° for (±)-**1**]. The energy profile of (−)-**1**, as determined by the CNDO/2[12] method, showed two stable B1 (ω = −110°) and B2 (ω = 110°) regions and two unstable P1 (ω = ca. −180°) and P2 (ω = −20—20°) regions; the same energy profile was also obtained for (±)-**1** (Fig. 6). The results indicate that **1** assumes an equilibrium state between the B1 and B2 rotamers and the energy barrier of P1 (= 6.2 kcal mol^{-1}) is too low to block the inter-conversion between the two rotamers. The torsion angles observed in the crystal structures of (−)-**1** and (±)-**1** are in the stable B1 and B2 regions, respectively.

On the other hand, the solution conformation of **1** was

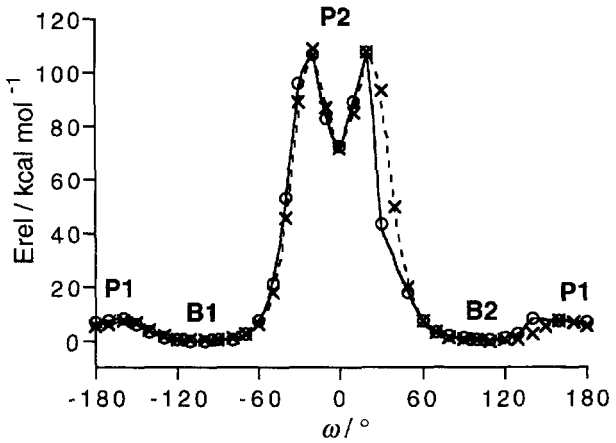

Fig. 6. Relative total energy profile as a function of torsion angle around the C17–C9–O3–C20 (ω) bond for (−)-**1** (X) and (±)-**1** (○). The relative total energy value was calculated based on the lowest energy of −174817.7634 kcal mol^{-1} for (−)-**1** and −174816.6394 kcal mol for (±)-**1**.

examined by the NMR spectroscopy of (−)-[N–$^{13}CH_3$]-**1** in C^2HCl_3. The NOE for H5b(C5)–H13(C13) proton pair suggested their close spatial arrangement on the α side of ring B, together with the solution conformation of ring B being essentially identical with that in the crystal structure of **1**: H5b–H13 = 2.1 Å for both (−)-**1** and (±)-**1**. NOESY spectrum revealed the orientation of the two methoxy groups on C9 and C10. For the orientation of the methoxy group on C10, NOE of the H11(C11)–H_3(C21) proton pair suggested a close spatial arrangement, coinciding with H11(C11)–H_3(C21) = 2.3 Å of (−)- **1** and (±)-**1** crystal structures. For the orientation of the methoxy group on C9, the NOE of H_3(C20)–H_3(C22) proton pair indicates the presence of B2 rotamer {H20c(C20)–H22a(C22) = 2.5 Å for (±)-**1**}(Fig. 7). However, the NOE with a relatively large intensity of H_2(C8)–H_3(C20) cannot discard the existence of rotamer B1 {i.e., the carbon atomic distance of C(8)–C(20) 3.370 Å for (−)-**1** and 3.656 Å for (±)-**1**)}. Therefore, the NMR results support the possibility of two rotamers, B1 and B2, in C^2HCl_3 solution at room temperature.

Rate of Racemization and Energy of (−)-1. The

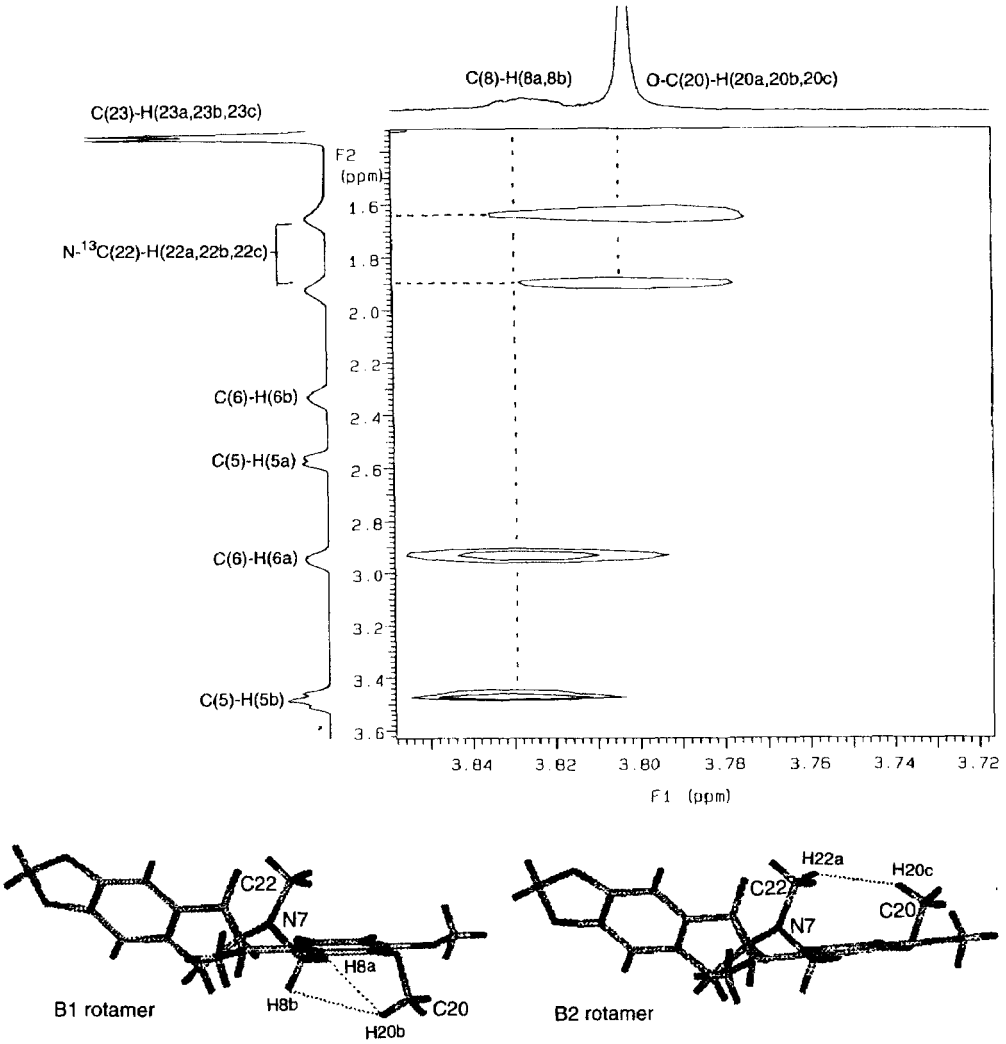

Fig. 7. Partial NOESY spectrum of (−)-[N–$^{13}CH_3$]-**1** observed at 23 °C in C^2HCl_3 solution. Significantly close spatial arrangements as NOEs in solution are indicated by dashed lines on B1 and B2 rotamers.

asymmetric C13 atom in the 13-methyl protopine-type alkaloid bears an ionizable hydrogen atom that is capable of racemization.[13] Thus, the racemization of (−)-**1** was monitored as a function of temperature. Measurements were carried out by MS spectrometry, taking advantage of the relatively high reactivity of C13–^{1}H for the exchange with ^{2}H in a deuterated solvent under alkaline conditions. The time courses of nondeuterated and deuterated species were monitored from the intensities at *m/z* 384 (M) and *m/z* 385 (M+1), respectively, where the experiments were performed at 1, 26, and 40 °C in $C^2H_3O^2H/NaO^2H$. The respective rates of racemization (k), which followed the first-order reaction, were obtained by least-squares analyses of the slopes: $k = 2.55\times10^{-2}$ min^{-1} ($t_{1/2}$ = 27.2 min) for 1 °C, 5.70×10^{-2} min^{-1} ($t_{1/2}$ = 12.2 min) for 26 °C, and 7.42×10^{-2} min^{-1} ($t_{1/2}$ = 9.4 min) for 40 °C. The activation energy (E_a = 4.7 kcal mol^{-1}) and frequency factor ($\log A$ = 5.0 min^{-1}) for the racemization were then estimated from the Arrhenius plot, where these values were obtained from the slope and intercept of the linear plot, respectively.

Discussion

In order to clarify the conformational/physicochemical properties of **1**, which are strongly related to the metabolic pathway of protoberberine-type alkaloids, (−)-**1** was biosynthesized using callus tissues of *C. majus*. Thermal analysis of (−)-**1** crystal revealed an irreversible transformation to the racemic crystal by heating, the latter crystal being energetically less stable than the former one. From this thermal behavior of **1**, the recrystallization of racemic (±)-**1** crystals led to two different polymorphisms: one is a racemic compound that exists as needle-like crystals {(±)-**1n**} with a homogeneous solid phase; the other is a conglomerate crystal in the form of prisms {(±)-**1p**}, which is a mechanical mixture of two pure (+)-**1** and (−)-**1** crystals.

The molecular conformation and crystal packing of (−)-**1** and (±)-**1n** were investigated by X-ray crystallographic analyses; the molecular structure of (±)-**1n** was the same as that of (−)-**1**. Consequently, nearly the same open conformation was observed in both crystal structures. These crystal structures were also shown to be preferred conformations by NMR measurements in a $CHCl_3$ solution.

We also estimated the racemization rate and the energy barrier for the transformation of (−)-**1** to (±)-**1**, based on the temperature dependence of the H⇔^{2}H exchange rate of C(13)–H of (−)-**1** in a deuterated solvent under alkaline conditions.

Based on the above-mentioned physicochemical properties of **1** in the enantiomeric and racemic forms, we consider the nonenzymatic epimerization at the C13 atom of a 13-methylprotopine-type alkaloid in vivo, as shown in Fig. 8. Because of the low-energy barrier (E_a = 4.7 kcal mol^{-1}) between (−)-(13*R*)-**1** and (+)-(13*S*)-**1**, various equilibrium ratios of (−)-1/(+)-**1** are possible at room temperature, depending on the culture condition and species. In general, the inversion of the absolute configuration on an asymmetric carbon in the skeleton necessitates an enzyme, such as a dehydrogenase/reductase or an epimerase, in the biosynthetic pathway of isoquinoline alkaloids.[14] However, the present study clearly suggests the possibility of a nonenzymatic interconversion between the (−)-(13*R*)- and (+)-(13*S*)-forms of the protopine-type alkaloid; also the ratio of the (13*R*)/(13*S*) enantiomers affects the natural abundance[15] of the final metabolite, (−)-(11*R*,13*S*,14*S*)/(+)-(11*S*,13*R*,14*R*)-hexahydrobenzo[*c*]phenanthridine alkaloid.

On the other hand, the preparation of a conglomerate crys-

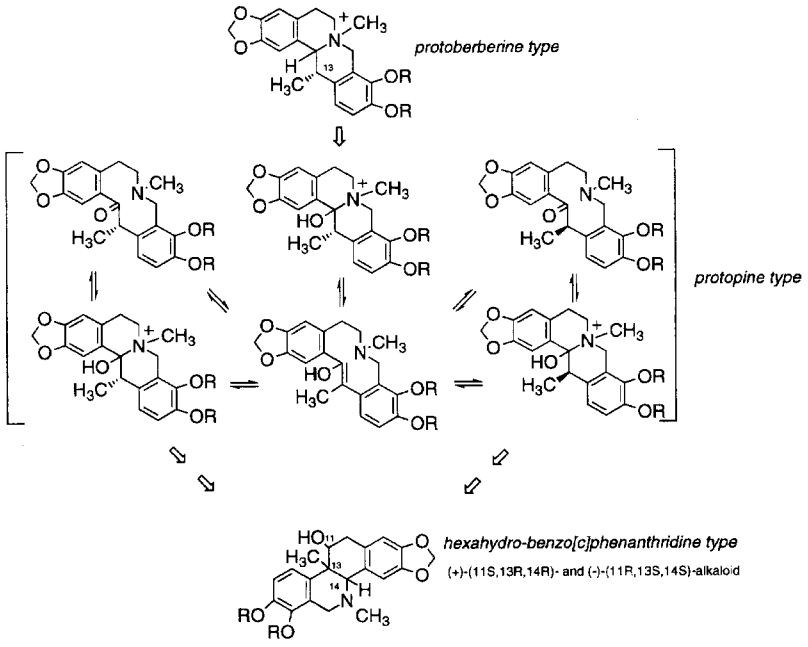

Fig. 8. Proposed biotransformation mechanism from an optically active protoberberine-type alkaloid to a racemic hexahydrobenzo-[*c*]phenanthridine-type alkaloid. Broad arrows: enzymatic reaction; narrow arrow: nonenzymatic reaction.

Table 1. Physicochemical Data for (−)-**1**, (±)-**1n**, (−)-**2**, and (±)-**2** Crystals

	(−)-**1**	(±)-**1n**	(−)-**2**	(±)-**2**
Melting point[a]/°C	212	193	146	217
Density[b]/g cm^{-3}	1.338	1.299	1.355	1.373
Volume[c] of unit cell[d]/Å^3	1899.4	1952.7	1795.4	1776.0
Volume per molecule[e]/Å^3	331.8	332.0	316.0	314.7
Energy calculations (MOPAC 6, PM3)				
Heat of formation/kcal mol (of a unit cell[d])	611.972	606.769		

a) The value was obtained by measurement with a microhot stage apparatus. b) The value was measured by the flotation method using an aqueous KI solution. c) The value was calculated with crystal data. d) Four molecules per a unit cell for (−)-**1**, (±)-**1n**, and (±)-**2**. Four molecules of two unit cells for (−)-**2**. e) The value was performed with 256 grids using "Volume Calculation" in MOL/MOLIS[18] system.

tal has been attracting increasing attention as a useful tool for the effective optical resolution of various synthetic agents. The present results would provide useful information concerning the relationship between the conglomerate/racemic crystal and the molecular packing energy (crystal structure stability). Since a rational explanation for preparing the conglomerate crystal is still unavailable, it appears important to consider the reason why (±)-**1** molecules lead to the formation of a conglomerate crystal (mechanical mixture of optically pure (−)-**1** and (+)-**1** crystals).

The formation of the conglomerate crystal and the racemic crystal means that the formation energy (packing energy) of the racemic crystal is equal to that of the enantiomeric crystal. In order to compare the stability of the crystal structures between (±)-**1** and (−)-**1**, some physicochemical data are summarized in Table 1, and the results for the crystal structures of (−)-**2**[10] and (±)-**2**[11] are also given for a comparison. The data indicate that the crystal structure of (−)-**1** is more stable than that of (±)-**1**. This contrasts with the expected result for **2**, where the crystal structure of (±)-**2** is more stable than that of (−)-**2**. On the other hand, the heat of formation, which was calculated for a crystal unit cell containing symmetry-related four molecules using the PM3 method[16] within MOPAC (v. 6),[17] does not agree with the physicochemical properties of the respective crystals. Based on these results, it could be said that the physicochemical properties of a crystal are dependent on the crystal packing. The heat of formation is very similar for the optically active and racemic crystals of **1** (ΔE = 5.203 kcal mol^{-1}), indicating that racemic and conglomerate crystals are formed at nearly the same frequency (energetic nonselectivity) in the case of (±)-**1**.

Since the molecular conformations of **1** and **2** enantiomeric and racemic crystals are very similar to each other, their notable physicochemical difference (Table 1) could be attributed to the substituent groups on C9 and C10. Owing to the methylenedioxyl group on the C9 and C10 atoms, the conformation of **2** is fixed and, consequently, the crystal packing environment differs significantly between (−)-**2**, and (±)-**2** crystals, leading to a notable difference in their physicochemical properties. In contrast, the polymorph of (±)-**1** could be attributed to the presence of flexible methoxy groups on the C9 and C10 atoms; i.e., any energetic inconvenience due to crystal packing could be compensated by the rotation of the methoxy group: energetically favored conformers of different torsion angles (C17–C9–O3–C20) were observed in the racemic and optically active crystals of **1**, respectively. This leads to the simultaneous appearance of racemic and conglomerate crystals.

Experimental

Melting points were taken on a microhot stage apparatus (MP-500D, Yanaco) and were uncorrected. Infrared (IR) absorption spectra were taken in KBr or $CHCl_3$ with a Hitachi 295 infrared spectrometer (FT-IR) at room temperature. Mass spectra were recorded on Hitachi M-80 double-focusing and M-4100 spectrometers equipped with an M-003 data processor, using the samples dissolved in aqueous solution. Optical rotations were measured using a JASCO-DIP-181 polarimeter. CD spectra were measured using a JASCO-J 720 spectropolarimeter. ^{1}H NMR spectra were measured in a C^2HCl_3 or $C^2H_3O^2H$ solution with tetramethylsilane (TMS) as an internal standard on a Gemini 300 (300 MHz) and a Varian VXR-500 (500 MHz) spectrometer. The NOESY spectrum was measured with a mixing time of 600 ms with 500 MHz.

Callus Culture. The callus was derived from the seedling root of *Chelidonium majus* (*Papaveraceae*) in the Botanical Garden University of Regensburg (Germany) and cultured on Murashige and Skoog's (M&S) medium[19] containing 2,4-dichlorophenoxyacetic acid (1 mg dm^{-3}), kinetin (0.1 mg dm^{-3}), and agar (1.0%). The callus tissues were subcultured in the dark every three weeks onto a fresh medium at 20 °C.

Biosynthetic Preparation of 1 and Spectral Data. To (±)-N–[$^{13}CH_3$]-**4** chloride[20] (300 mg) was added sterilized water (30 ml); 2 ml aliquots of this aqueous solution were poured into 100 ml Erlenmeyer flasks containing callus (10 g, three weeks old) in the M & S medium (40 ml). The cultures were incubated in the dark on a rotary shaker (125 rpm) at 20 °C for seven days. The cells and the medium were separated by filtration through a thin cotton cloth. In the conventional way,[7] **1** (11.8 mg) was isolated from cells and medium fractions. Other experimental results are given in Table 2. **1**; R_f = 0.25 (methanol). Mp 209.0—210.0 °C (acetone). [α_D] −219.5° (c = 0.4, $CHCl_3$). IR ν_{max} 1668 cm^{-1} (C=O). Mass *m/z*: Calcd for $^{13}C \cdot C_{21}H_{25}NO_5$: M^+, 384.1767. Found: *m/z* 384. CD [θ] {0.998 mM (1 M = 1 mol dm^{-3}) in methanol, L = 0.089 mm} 298.90 nm -4.934×10^3, 280.20 nm 8.863×10^3, 255.90 nm -2.947×10^4, 239.00 nm -1.895×10^4, 226.00 nm 1.705×10^4, 205.80 nm -1.023×10^5. ^{1}H NMR (C^2HCl_3) δ = 7.091 (1H, *d*, J = 8.5 Hz, C12–H), 7.016 (1H, *s*, C1–H), 6.892 (1H, *d*, J = 8.5 Hz, C11–H), 6.660 (1H, *s*, C4–H), 5.961 (2H, *d.d*, J = 11.0, 1.5

Table 2. Biotransformation of **1** by Suspension Cultures of *Chelidonium majus* (*C.m.*), *Corydalis incisa* (*C.i.*), *C. ochotensis* (*C.o.*) and *Macleaya cordata* (*M.c.*)

Ex.No.	Cell (fr.wt. g)	Substrate (mg)	Incubation period (day)	Transformation yield[a] of **1**(%)
1	*C.m.* (134)	4 (100.0)	12	3.9
2	*C.m.* (77)	4 (101.1)	10	3.8
3	*C.m.* (163)	4 (140.2)	7	4.1
4	*C.m.* (205)	4′ (100.0)	12	1.5
5	*C.i.* (72)	4 (105.7)	10	1.4
6	*C.i.* (81)	4 (106.7)	12	1.0
7	*C.i.* (122)	4′ (91.7)	12	0.5
8	*C.o.* (107)	4 (100.5)	10	tr
9	*C.o.* (164)	4′ (100.2)	11	n.d.
10	*M.c.* (161)	4 (100.7)	11	n.d.
11	*M.c.* (163)	4′ (96.0)	11	n.d.

Abbreviations; fresh weight = fr.wt., tr = detected but not quantified, n.d. = not detectable. **4**; (±)-[N–$^{13}CH_3$]-*meso*-thalictricavinium chloride, 4′; (±)-[N–$^{13}CH_3$]-thalictricavinium chloride. a) Transformation yield = mole of **1**/mole of substrate × 100.

Hz, C19–H_2), 4.183 (1H, *q*, *J* = 7.0 Hz, C13–H), 3.878 (3H, *s*, C21–H_3), 3.836 (2H, *b.s*, C8–H_2), 3.803 (3H, *s*, C20–H_3), 3.484 (1H, *b.t*, *J* = ca. 15, 2 Hz, C5–H), 2.937 (1H, *b.d*. *J* = ca. 13, 2 Hz, C6–H), 2.557 (1H, b.d, *J* = ca. 15, 2 Hz, C5–H), 2.297 (1H, *b.t*, *J* = ca. 13, 2 Hz, C6–H), 1.787 (3H, *d*, *J* = 134.0 Hz, N–$^{13}CH_3$), 1.345 (3H, *d*, *J* = 7.0 Hz, C23–H_3). NOESY Cross-peak (C^2HCl_3); C(12)–H→C(23)–H_3, C(11)–H; C(11)–H→C(12)–H,C-(21)–H_3; C(4)–H→C(5)–H(5a); C(13)–H→C(8)–H(8b), C(5)–H-(5b), C(23)–H_3; C(21)–H_3→C(11)–H; C(8)–H(8b)→C(13)–H, C(20)–H_3, C(5)–H(5b), C(6)–H(6a); C(20)–H_3→C(22)–H_3; C(5)–H(5b)→C(13)–H, C(8)–H(8b), C(5)–H(5a); C(6)–H(6a)→C-(13)–H, C(8)–H(8b), C(5)–H(5a), C(6)–H(6b); C(5)–H(5a)→C-(4)–H, C(5)–H(5b); C(6)–H(6b)→C(6)–H(6a); C(22)–H_3→C-(20)–H_3; C(23)–H_3→C(12)–H, C(13)–H.

Thermal Analysis. DSC thermograms of the sample were recorded on a differential scanning calorimeter (DSC 7, Perkin–Elmer) connected to a DEC Venturis 466 computer (EPSON). The system was able to calculate the extrapolated onset temperature, peak temperature and enthalpy values for each thermal reading. The temperature axis was calibrated with pure indium (mp 156.60 °C). 1.338 mg of (−)-**1** on an aluminum cell as a sample container was examined. Heating rates (5.0 °C min^{-1}) and nitrogen gas flow rates (30 ml min^{-1}) were varied according to the purpose of the experiment.

TG was performed using a thermogravimetric analyzer (TGA 7, Perkin–Elmer). The operating conditions in an open-pan system were as follows: sample weight on an aluminum cell, 1.953 mg; heating rate, 5 °C min^{-1}; and N_2 gas flow rate, 30 ml min^{-1}.

Measurement of Racemization Rate of (−)-1. In a 5 ml-test tube was dissolved (−)-**1** (1 mg) in $C^2H_3O^2H$ (2 ml) with stirring; the test tube was maintained at bath temperatures of 1, 26, and 40 °C during the reaction. After the addition of NaO^2H (0.025 mol dm^{-3}, 0.66 ml) into the tube, 100 μl portions of the reaction mixture were sampled from 0 to 60 min. Each sample was dried almost immediately with N_2 gas. Mass measurements of the sample (as a solution of CH_3CN) were made using the EI method (beam energy 70 eV, positive mode). The percentage of residual (−)-**1** was calculated based on the intensity values at the molecular ion peak of **1** *m/z* 384 and deuterated species of **1** *m/z* 385, as intensity of 384 × 100/intensity of (384 + 385 + isotope peak of natural abundance of 384), and the slope was determined by the least squares method.

Preparation of (±)-1. (−)-**1** (40 mg) was dissolved in a mixture of MeOH (80 ml) and NaOH solution (0.025 mol dm^{-3}, 25 ml) and stirred at 70 °C. After 3 h, the solution was evaporated in vacuo and $CHCl_3$ (50 ml) was added to the residue. The $CHCl_3$ layer was washed with sat. NaCl solution, dried (K_2CO_3), and evaporated to give 36.8 mg of (±)-**1**, as powder. mp 193.2—194.0 °C (acetone/ether); $[\alpha]_D$ 0° (*c* = 0.25, $CHCl_3$).

Recrystallization of (±)-1 from Acetone Solution. (±)-**1** (40 mg) was dissolved in acetone (40 ml) and aliquots of 10 ml of this solution were poured into four 20 ml beakers. Upon standing for 8 d at approx. 25 °C, two types of crystals formed: needlelike (**1n**) in three beakers and prismatic (**1p**) in one beaker; **1n**, mp 193.2—194.0 °C (acetone); **1p**, mp 209.0—210.0 °C (acetone).

Optical Resolution of (±)-1p Crystals. The prismatic crystals (**1p**) that were formed in one of the four beakers were observed under a microscope [200 magnification] using polarized light. Under the microscope, all of the crystals in the beaker were divided into 31 fractions: single crystals were isolated while large crystals, apparently not single ones, were divided by the tip of an injection needle. The optical rotational all 31 fractions in $CHCl_3$ were measured using a microcell (cell length of 50 mm). Fr.No.1; $[\alpha]_D$ −88.9° (*c* = 0.009), Fr.No.2; $[\alpha]_D$ +149.2° (*c* = 0.063), Fr.No.3; $[\alpha]_D$ +200° (*c* = 0.009), Fr.No.4;$[\alpha]_D$ −133.3° (*c* = 0.009), Fr.No.5; $[\alpha]_D$ +93.3° (*c* = 0.060), Fr.No.6; $[\alpha]_D$ −100.0° (*c* = 0.066), Fr.No.7; $[\alpha]_D$ +202.2° (*c* = 0.064), Fr.No.8; $[\alpha]_D$ −94.5° (*c* = 0.055), Fr.No.9; $[\alpha]_D$ +106.5° (*c* = 0.062), Fr.No.10; $[\alpha]_D$ −108.2° (*c* = 0.061), Fr.No.11; $[\alpha]_D$ −131.1° (*c* = 0.61), Fr.No.12; $[\alpha]_D$ −210.1° (*c* = 0.080), Fr.No.13; $[\alpha]_D$ −139.7° (*c* = 0.063), Fr.No.14; $[\alpha]_D$ +177.8° (*c* = 0.009), Fr.No.15; $[\alpha]_D$ −142.9° (*c* = 0.007), Fr.No.16; $[\alpha]_D$ +50.9° (*c* = 0.055), Fr.No.17; $[\alpha]_D$ −60.0° (*c* = 0.010), Fr.No.18; $[\alpha]_D$ 0° (*c* = 0.009), Fr.No.19; $[\alpha]_D$ +60.0° (*c* = 0.010), Fr.No.20; $[\alpha]_D$ +63.2° (*c* = 0.057), Fr.No.21; $[\alpha]_D$ −66.7° (*c* = 0.009), Fr.No.22; $[\alpha]_D$ −57.1° (*c* = 0.007), Fr.No.23; $[\alpha]_D$ −44.4° (*c* = 0.009), Fr.No.24; $[\alpha]_D$ −80.6° (*c* = 0.062), Fr.No.25; $[\alpha]_D$ +50.0° (*c* = 0.008), Fr.No.26; $[\alpha]_D$ −42.1° (*c* = 0.057), Fr.No.27; $[\alpha]_D$ 0° (*c* = 0.008), Fr.No.28; $[\alpha]_D$ −40.0° (*c* = 0.010), Fr.No.29; $[\alpha]_D$ 0° (*c* = 0.010), Fr.No.30; $[\alpha]_D$ −40.0° (*c* = 0.010), Fr.No.31; $[\alpha]_D$ −66.7° (*c* = 0.069).

X-Ray Crystal Structure Determination. Single crystals of (−)-**1**, (+)-**1**, and (±)-**1n** were crystallized from acetone at room temperature. Single crystals of (−)-**1** and (+)-**1** were both obtained as transparent prisms and the single crystal of (±)-**1n** was

Table 3. Summary of Crystal Data and Details of Intensity Collection

	(±)-**1n**	(−)-**1**	(+)-**1**
Formula	$^{13}C{\cdot}C_{21}H_{25}NO_5$	$^{13}C{\cdot}C_{21}H_{25}NO_5$	$^{13}C{\cdot}C_{21}H_{25}NO_5$
Mr	384.43	384.43	384.43
Crystal system	Monoclinic	Orthorhombic	Orthorhombic
Space group	$P2_1/n$	$P2_12_12_1$	$P2_12_12_1$
a/Å	12.090(2)	11.915(2)	11.920(2)
b/Å	11.467(2)	14.962(2)	14.974(2)
c/Å	14.644(2)	10.654(2)	10.649(2)
β/Å°	105.89(1)	90.00	90.00
V/Å^3	1952.7(4)	1899.4(5)	1900.7(5)
Z	4	4	4
D_m/g cm^{-3}	1.299 (4)	1.338(4)	1.340(5)
D_x/g cm^{-3}	1.304	1.341	1.340
μ(Cu $K\alpha$)/mm^{-1}	0.76	0.78	
F(000)	816	816	
T of data collection/°C	20	20	
Scan speed in 2θ/° min^{-1}	12	12	
Scan range in ω/°	1.150+0.15 tan θ	1.68+0.15 tan θ	
No. of unique data measured	3080	1724	
No. of data used for refinement	2132 [$I > 2\sigma(I)$]	1664 [$I > 2\sigma(I)$]	
No. of variables	253	253	
$R1$	0.046	0.047	
$wR2$	0.123	0.119	
S	1.041	0.616	

obtained as transparent needles. Single crystals of dimensions of 0.3×0.1×0.5 mm for (±)-**1n**, 0.9×0.3×0.5 mm for (−)-**1**, and 0.3×0.3×0.2 mm for (+)-**1** were used for X-ray diffraction studies on a Rigaku AFC-5 diffractometer employing graphite-monochromated Cu $K\alpha$ radiation. A summary of the crystallographic data[9] is given in Table 3. The unit-cell dimensions were determined by a least-squares fit of 2θ angles for 25 reflections of $20° \leq 2\theta \leq 40°$. The crystal density was measured by a flotation method using an aqueous KI solution. The intensity data within 2θ = 130° were collected with the ω–2θ scan mode at 20 °C, where the backgrounds were counted for 5 s at both extremes of each reflection peak. Four standard reflections were monitored at 100 reflection intervals throughout the data collection, showing a random variation of < ±1% without any significant trends. The observed intensities were corrected for Lorentz and polarization effects, and no absorption correction was made.

The structure was solved by direct methods using the MULTAN program.[21] The positional parameters of non-H atoms were refined by a full-matrix least-squares method with isotropic thermal parameters, and then with anisotropic thermal parameters {SHELXL-93 program[22]}. The geometrically ideal positions of H atoms were calculated and included in a calculation of the structure factors. The function of $\Sigma w(F_o^2 - F_c^2)^2$ was minimized, and $w = [\sigma(F_o^2)^2 + (0.1412p)^2 + 10.69p]^{-1}$ for (±)-**1n** and $w = [\sigma(F_o^2)^2 + (0.1376p)^2 + 16.58p]^{-1}$ for (−)-**1** were used, where $p = (\mathrm{Max}(F_o^2, 0) + 2F_c^2)/3$. Final $R1$ [$(\Sigma||F_o| - |F_c||/\Sigma|F_o|]$, $wR2$ $[(\Sigma w(F_o^2 - F_c^2)^2/\Sigma w(F_o^2)^2)^{1/2}]$ and S $[(\Sigma w(F_o^2 - F_c^2)^2/(M - N))^{1/2}$, where M = no. of reflections with $F_o^2 > 2\sigma(F_o^2)$ and N = no. of variables used for the refinement] are also given in Table 3. None of the positional parameters of non-H atoms shifted by more than one-third from their estimated standard deviations for both compounds, and the unassigned electron density in the final stage of the refinement was in the range of −0.250 to 0.207 Å^{-3} for (±)-**1n** and −0.401 to 0.276 Å^{-3} for (−)-**1**. The atomic scattering factors and terms of anomalous dispersion corrections were taken from literature.[23] Tables of the final atomic coordinates of non-H atoms, anisotropic thermal parameters of non-hydrogen atoms, bond lengths, bond angles and torsion angles (21 pages) are deposited as Document No.73026 at the Office of the Editor of Bull. Chem. Soc. Jpn. All numerical calculations were carried out at the Computer Center, Osaka University of Pharmaceutical Sciences. Crystallographic data have been deposited at the CCDC, 12 Union Road, Cambridge CB2 1EZ, UK and copies can be obtained on request, free of charge, by quoting the publication citation and the deposition numbers 140358-140360.

Molecular Orbital Calculations. The total energies for various conformers of **1** were calculated using the CNDO/2 method,[12] as a function of torsion angle around the C(17)–C(9)–O(3)–C(20) (ω) bond. The atomic coordinates of (−)-**1** and (±)-**1n** were used from the present X-ray results for the calculation. The stability of the electronic energy was used as a check for convergence in the iteration calculation. The total energies (kcal mol^{-1}) of different rotamers were computed in increments of 10° of the ω angle from −180° to 180°, where the structure was not optimized at each of the torsion angles, because the ratable bonds are limited to the methyl groups.

Energy Calculations of Heat of Formation. The heat of formations of (−)-**1** and (±)-**1n** were calculated on a 4D Indy using MOPAC v.6[17] (AM3)[16] in MOL/MOLIS[18] system. The atomic coordinates of (−)-**1** and (±)-**1n** were used from the present X-ray results. Four molecules of (−)-**1** and (±)-**1n** were built up by symmetry operations of $P2_12_12_1$ and $P2_1/n$, respectively.

This research was supported in part by the *Alexander von Humboldt-Stiftung* of Germany. M.K. wishes to thank Professor Dr. W. Wiegrebe for supplying the materials for callus cultures and for his interest in this work.

References

1 M. Kamigauchi and K. Iwasa, "Biotechnology in Agriculture and Forestry, Vol. 26 Medicinal and Aromatic Plants VI," ed by Y. P. S. Bajaj, Springer-Verlag, Berlin (1994), p. 93.

2 The atomic numbering for **1** is due to the convention of the field of alkaloid.

3 J. Gadamer, *Arch. Pharm.*, **249**, 30 (1911).

4 F. v. Bruchhausen, *Arch. Pharm.*, **263**, 570 (1925).

5 M. Kamigauchi, Y. Noda, K. Iwasa, Z. Nishijo, T. Ishida, Y. In, and W. Wiegrebe, *Helv. Chim. Acta*, **77**, 243 (1994).

6 N. Takao, M. Kamigauchi, and M. Okada, *Helv. Chim. Acta*, **66**, 473 (1983).

7 M. Kamigauchi, Y. Noda, K. Iwasa, N. Takao, and W. Wiegrebe, *Arch. Pharm. (Weinheim)*, **325**, 585 (1992).

8 J. Jacques, A. Collet, and S. H. Wilen, "Enantiomers, Racemates, and Resolutions," Krieger Publishing Comp, Malabar (1994), p. 43.

9 Crystalline particles, which show opposite signs, were separately collected and recrystallized in acetone at room temperature. Transparent prismatic crystals appeared from the respective solutions after several days. CD spectra indicated 100% optical purity. Comparison of the crystal data between (+)-**1** and (−)-**1** gave excellent agreement within experimental error, indicating that the crystal structure of (+)-**1** could be regarded as the antipodal form of (−)-**1** with the same molecular packing in the crystal. Therefore, the crystal structure analysis of (+)-**1** was not described in detail in this paper.

10 M. Kamigauchi, Y. Noda, K. Iwasa, Z. Nishijo, N. Takao, T. Ishida, Y. In, and M. Inoue, *Arch. Pharm. (Weinheim)*, **326**, 501 (1993).

11 M. Kamigauchi, K. Iwasa, N. Takao, T. Ishida, and M. Inoue, *Helv. Chim. Acta*, **70**, 1482 (1987).

12 J. A. Pople and G. A. Segal, *J. Chem. Phys.*, **44**, 3289 (1966).

13 A. K. Mills and A. E. W. Smith, *Helv. Chim. Acta*, **43**, 1915 (1960).

14 A. R. Battersby, D. M. Foulkes, M. Hirst, G. V. Parry, and J. Staunton, *J. Chem. Soc. C*, **1968**, 210.

15 N. Takao, M. Kamigauchi, and K. Iwasa, *Tetrahedron*, **35**, 1977 (1979).

16 J. J. P. Stewart, *J. Comput. Chem.*, **10**, 209 (1989).

17 J. J. P. Stewart, *QCPE* #455.

18 "MOL/MOLIS; Molecular Orbital Analysis System," Daikin Industries, Ltd.

19 T. Murashige and F. Skoog, *Physiol. Plant*, **15**, 473 (1962).

20 K. Iwasa, M. Sugiura, and N. Takao, *J. Org. Chem.*, **47**, 4275 (1982).

21 P. Main, S. E. Hull, L. Lessinger, G. Germain, J. P. Declercq, and M. M. Woolfson, "MULTAN 78, A System of Computer Programs for the Automatic Solution of Crystal Structures from X-ray Diffraction Data," Universities of York and Louvain, Belgium (1978).

22 G. M. Sheldrick, "SHELX-93, A Program of the Refinement of Crystal Structures from X-ray Diffraction Data," University of Goettingen, 1993.

23 "International Tables for X-Ray Crystallography," Kluwer Academic Publishers, Dordrecht (1992), Vol. C.